

# Micromagnetics of the dynamic susceptibility for coupled permalloy stripes

O. Gérardin, J. Ben Youssef, H. Le Gall

*Laboratoire de Magnétisme de Bretagne, UMR CNRS 6135, Université, 29285 Brest, France*

N. Vukadinovic, P.M. Jacquart

*Dassault Aviation, 92552 St Cloud, France*

M. J. Donahue

*National Institute of Standards and Technology, Gaithersburg, MD 20899, USA*

(October 18, 2000)

## Abstract

The dynamic susceptibility of arrays of narrow permalloy stripes ( $9\text{ mm} \times$  several  $\mu\text{m} \times 200\text{ nm}$ ) has been investigated using a single-coil broadband susceptibility spectrometer. Disagreement is observed between experimental results and the macroscopic Landau-Lifshitz (LL) model. This model does not take into account the dipolar interaction between magnetic stripes. We have performed micromagnetic calculations that include these dipolar interactions, and have found the resulting frequency dependence of the dynamic susceptibility in the linear regime to be in good agreement with our experimental data.

## I. INTRODUCTION

Fine control of the magnetic susceptibility in the high frequency range (100 MHz – 10 GHz) is required for many industrial applications. For example, obtaining short switching times for magnetic recording applications requires high cut-off frequencies of the real part of the dynamic susceptibility. For other applications, such as microwave devices, fine control of the resonance frequency of the uniform gyromagnetic mode may be needed. There are many ways to change the gyromagnetic resonance frequency for a given material experimentally, such as using DC applied magnetic fields, thermomagnetic treatments [1] or patterning [2,3]. In this work, the last method has been used: laser ablation is used to pattern thin permalloy films into arrays of long stripes parallel to the easy axis of magnetization. Then, measurements of the dynamic susceptibility is performed on the patterned films. The main effect of such a patterning is to raise the resonance frequency by inducing demagnetizing fields. Usually, the macroscopic Landau-Lifshitz (LL) model is used to explain the results, with a simple evaluation of the demagnetizing fields. In spite of good qualitative results obtained by this method, it is unable to take into account either the non-uniformity of the demagnetizing field in the sample, or the interactions between stripes. The interaction between stripes could be taken into account with effective medium theory. One can find more references in [4]. One alternative to this calculations is to use a micromagnetic description of the problem. In this paper, we have used a micromagnetic calculation to determine the dynamic susceptibility in the gigahertz range.

## II. EXPERIMENTAL DEVICES

### A. Material and ablation facility

The films are made of permalloy, grown by rf sputtering with Leybold-Heraeus equipment. They were deposited onto a 9 mm  $\times$  9 mm Corning glass substrate. The thickness of the magnetic layer is 200 nm. B-H loop cycles show a well defined uniaxial anisotropy for the

as-sputtered films. The magnetic properties of the as-sputtered films were determined using a vibrating sample magnetometer (VSM). The films were patterned into stripes parallel to the easy axis of magnetization with a simple laser ablation facility described elsewhere [3]. Several depositions were made in order to realize different patterns. We have made arrays of 9 mm length ( $l$ ), 50, 75 and 100  $\mu\text{m}$  width ( $w$ ), separated by 10  $\mu\text{m}$ , in order to maintain arrays with a high area packing fraction respectively from 83% up to 90%. There are between 80 and 150 stripes, depending on the width. The thickness is identical for all structures, equal to 200 nm.

### **B. Magnetic susceptibility measurements**

The dynamic magnetic susceptibility of the samples was investigated using a permeameter based on the measurement of the reflexion parameter of a single coil [5,6] without/with the magnetic film. Using this permeameter and an HP 8753-a vectorial network analyzer, the susceptibility can be measured in the 30 MHz to 6 GHz frequency range. The configuration of the measurement is described in Fig. 1. For the patterned samples, the magnetic excitation field  $\mathbf{h}(t)$  was applied perpendicular to the length of the stripe, in the film plane. The patterning induces a shift of the gyromagnetic resonance frequency to higher values and decreases the susceptibility. Typical spectra are reported in Fig. 2. These results can be understood simply by the fact that the patterning increases the shape anisotropy of the film by inducing demagnetizing fields.

## **III. THEORETICAL APPROACHES**

### **A. Macroscopic Landau-Lifshitz Model**

The dynamic behavior of the magnetization is usually described with the help of the Landau-Lifshitz macroscopic model. This model explains dynamic behavior under the assumption that the magnetization configuration is uniform. In this model, the temporal

evolution of the magnetization  $\mathbf{M}$  is:

$$\frac{d\mathbf{M}}{dt} = -|\gamma|\mathbf{M} \times \mathbf{H} - \frac{\alpha\gamma}{|\mathbf{M}|}\mathbf{M} \times [\mathbf{M} \times \mathbf{H}]. \quad (1)$$

Here  $\mathbf{H}$  is the total field,  $\gamma$  the gyromagnetic ratio,  $\alpha$  the phenomenological damping constant. Usually this equation is solved after linearization, using an harmonic excitation  $\mathbf{h}(t)$  of small amplitude, included in the total field  $\mathbf{H}$ . In the macroscopic LL model, if we take the ( $Ox$ ) axis along the length, and if we probe the susceptibility perpendicular to this axis, and in the plane of the film (see Fig. 1), the susceptibility is given by:

$$\chi(\omega) = -\frac{M_s\gamma^2(j\omega\frac{\alpha}{\gamma} + (H_k + M_sN_z))}{\omega^2 - j(2H_k + M_s(1 - N_x))\omega\alpha\gamma - (H_k + M_sN_y)(H_k + M_sN_z)(1 + \alpha^2)\gamma^2}, \quad (2)$$

where  $M_s$  is the saturation magnetization,  $H_k$  the anisotropy field,  $N_\alpha$  the demagnetization coefficient along the  $\alpha = \{x, y, z\}$  axis, and  $\omega$  the frequency.  $N_x$  is neglected, since the length of the sample is large compared to the thickness. Demagnetizing fields are homogenous only for ellipsoids, and can be defined by the demagnetizing factors:  $\mathbf{H}_d = -\overline{\overline{N}} \cdot \mathbf{M}$ . For all other geometries, the non-uniformity of the demagnetization pattern should be taken into account for the determination of demagnetizing fields, and we cannot write the demagnetizing fields in terms of tensorial demagnetizing factors. But in [7], the authors give a perturbative calculation of the demagnetizing fields. To first order, the demagnetization coefficients can be analytically derived in each point of the sample, and because it is a first order correction, we can still write the demagnetizing fields in terms of tensorial demagnetizing factors. In this way we can use the macroscopic LL model even if our stripes are not second order geometries. In Fig. 3 we see the variation along the ( $Ox$ ) axis of  $N_z$  for a  $10 \mu\text{m} \times 9 \text{mm} \times 200 \text{nm}$  structure. To introduce such a coefficient into the macroscopic LL model, we have to perform a spatial integration. The demagnetizing coefficients then become:

$$N_z = \int_V \frac{1}{4\pi} \sum_{i=1}^2 \sum_{j=1}^2 \sum_{k=1}^2 \cotan^{-1} f [(-1)^i x, (-1)^j y, (-1)^k z] d\vec{r} \quad (3)$$

with:

$$f(x, y, z) = \frac{((a-x)^2 + (b-y)^2 + (c-z)^2)^{\frac{1}{2}}(c-z)}{(a-x)(b-y)}. \quad (4)$$

The other components of the demagnetizing tensor are obtained by circular permutation of  $\{x, y, z\}$  and  $\{a, b, c\}$  in the two above expressions. This may be the best first order correction to the macroscopic LL model that takes into account the non-uniformity of the demagnetizing fields.

## B. Micromagnetic calculations

Instead of solving a macroscopic Landau-Lifshitz equation, a micromagnetic description of the problem can be used. In this work the OOMMF code from NIST was used. In the micromagnetic framework [8,9], the magnetization distribution is obtained by the minimization of the total energy density functional:

$$E = E_{\text{exch}} + E_{\text{demag}} + E_{\text{anis}} + E_{\text{zeeman}}. \quad (5)$$

The average energy density  $E$  is a function of  $\mathbf{M}$  and includes exchange, demagnetization, anisotropy and applied field (Zeeman). The exchange is calculated by an 8-neighbor interpolation:  $E_{\text{exch}}^i = (A/3) \sum_{j=1}^8 (1 - \mathbf{m}_i \cdot \mathbf{m}_j)$ . The magnetostatic fields are calculated with FFT techniques. One can find more details about the program and the evaluation of the energy terms in [10,11]. The time evolution of the magnetization distribution is determined by solving a microscopic Landau-Lifshitz equation, in which the effective field is a function of time and position:

$$\frac{\partial \mathbf{M}(\mathbf{r}, t)}{\partial t} = -|\gamma| \mathbf{M}(\mathbf{r}, t) \times \mathbf{H}_{\text{eff}}(\mathbf{r}, t) - \frac{\alpha \gamma}{|\mathbf{M}|} \mathbf{M}(\mathbf{r}, t) \times (\mathbf{M}(\mathbf{r}, t) \times \mathbf{H}_{\text{eff}}(\mathbf{r}, t)) \quad (6)$$

$$\mathbf{H}_{\text{eff}} = -\frac{1}{\mu_0} \frac{\partial E}{\partial \mathbf{M}}. \quad (7)$$

Starting in an equilibrium state, the susceptibility is obtained by exciting the system with a small external field having a time dependence that allows us to investigate the susceptibility in the correct range. This field is spatially homogeneous and is introduced in the density functional of the Zeeman term. The amplitude of the driving field is very small to minimize non-linear behavior. We define the spatial average susceptibility in the direction  $\mathbf{u}$  as:

$$\langle \mathbf{M}(t) \rangle \cdot \mathbf{u} = \int_{-\infty}^{+\infty} \chi(t-t') [\mathbf{h}(t') \cdot \mathbf{u}] dt', \quad (8)$$

where

$$\langle \mathbf{M}(t) \rangle = \frac{1}{V} \int_V \mathbf{M}(\mathbf{r}, t) d\mathbf{r}. \quad (9)$$

Performing FFT's on the excitation and the response, the obtained expression of the susceptibility can be directly compared to the one obtained by the macroscopic LL model (formula 2). In our calculations, since the stripes are very long, we assume one invariant direction for the magnetization. If we write the magnetization in the form  $\mathbf{M}(x, y, z)$ , we assume that the magnetization does not depend on  $x$ , where  $x$  is directed along the length of the stripe. The main drawback of this assumption is that the flux closure domains at the ends of the structure are neglected. However, we expect that the contribution of such domains to the susceptibility is very small. The mesh size used for the calculation is  $10 \mu\text{m}$  in the  $(y, z)$  plane.

#### IV. EXPERIMENTAL SUSCEPTIBILITY RESULTS AND ANALYSIS

First, the experimental spectra for the as-sputtered films are compared with the theoretical predictions deduced from the macroscopic LL model (Fig. 4). The parameters ( $H_k, M_S$ ) determined by static measurements are introduced to the model and we fit the damping parameter  $\alpha$ . Good agreement between measurement and theoretical predictions is found as observed in Fig. 4.

Second, the patterned films are considered. Table I reports resonance frequencies, both experimental and as predicted by the macroscopic LL model, for stripe widths of 50, 75 and  $100 \mu\text{m}$ . The the macroscopic LL model results are higher than those experimentally measured, and the discrepancy increases with stripe width. As mentioned above, the stripes are not as independent. To take into account the interaction between stripes, and to include a finer evaluation of the demagnetizing field, micromagnetic calculations are performed. The first calculations are performed in order to point out the influence of the number of

stripes on the dynamic susceptibility. We have considered 50  $\mu\text{m}$  stripes of ideal permalloy ( $M_s=800 \text{ kA}\cdot\text{m}^{-1}$ ,  $H_k=500 \text{ A}\cdot\text{m}^{-1}$ ), separated by 10  $\mu\text{m}$  non-magnetic spacers. Starting from one calculated stripe up to 8 stripes, the results of the influence of the number of stripes on the resonance frequency for the gyromagnetic mode is plotted in Fig. 5. The magnetostatic interaction between stripes reduces the demagnetizing fields. The frequency tends to an asymptotic value as the number of interacting stripes is increased. The shift of the frequency between 6 and 8 stripes is less than 50 MHz for this calculation.

We use the experimental magnetic parameters ( $H_k, M_s, \alpha$ ) of each sample before patterning to predict the susceptibility of patterned layers by micromagnetic calculations. In Fig. 6 we plot the frequency of the gyromagnetic resonance for experimental data, macroscopic LL model and micromagnetic calculations for 1 stripe and for 6 stripes. The discrepancy between the experimental results and macroscopic LL is due mainly to the interactions that are neglected in that model. The evaluation of the demagnetizing fields using a first order approximation in the macroscopic LL model seems to explain fairly well the behavior of an isolated stripe. The frequency obtained by micromagnetic calculations for one stripe is very similar to that obtained by the macroscopic LL model. As we see in Fig. 6, the macroscopic LL model is better for the largest aspect ratio ( $l/w$ ), which may be simply explained by the fact that the non-uniformity of the demagnetizing field is greatest near the boundaries.

The imaginary part of the susceptibility is plotted in Fig. 7, for the array of 75  $\mu\text{m}$  wide stripes: experimental after patterning, macroscopic LL model prediction, and micromagnetic calculation for 6 stripes. One can see the broadening of the experimental spectrum for the layer after patterning. This broadening may be caused by defects produced by the process of laser ablation, but we do not have a simple explanation for why the broadening affects only the low frequency part of the spectra. We see here that the micromagnetic calculation provides a better description of the susceptibility than the macroscopic LL model.

## V. CONCLUSION

In this work, the influence of the interaction between permalloy stripes on the magnetic susceptibility spectrum is investigated. The macroscopic LL model successfully explains the dynamic behavior of simple magnetic structures, but does not predict accurately the response of coupled structures. To circumvent this problem, it has been shown that micromagnetic calculations can be performed with success. A good agreement between experimental data and simulations is achieved. Such a micromagnetic determination of the susceptibility may be useful for predicting the behavior of complicated magnetic structures, such as multilayers, where there is no analytic method for calculating the susceptibility.

## TABLES

TABLE I. Gyromagnetic mode frequency: macroscopic LL model and experimental measurements.

stripe width ( $\mu\text{m}$ ):	50	75	100
frequency (experiment, GHz):	1.9	1.4	1.1
frequency (macroscopic LL model, GHz):	2.1	1.7	1.5

## REFERENCES

- [1] O. Acher *et al.*, IEEE Trans. Magn. **32**, (1996).
- [2] G. Perrin, J. Peuzin, and O. Acher, J. Appl. Phys. **81**, (1997).
- [3] H. LeGall, J. Gouzerh, and J. B. Youssef, J. Appl. Phys. **81**, (1997).
- [4] J. P. Bouchaud and P. G. Zérah, Phys. Rev. Lett. **63**, 1000 (1989).
- [5] D. Pain *et al.*, J. Appl. Phys. **85**, (1999).
- [6] V. Korenivski *et al.*, IEEE Trans. Magn. **32**, 4905 (1996).
- [7] R. Joseph and E. Schlomann, J. Appl. Phys. **36**, (1965).
- [8] W. Brown, *Micromagnetics* (North Holland, 1962).
- [9] M. E. Shabes, Journal of Magnetism and Magnetic Materials **95**, 249 (1991).
- [10] R. D. McMichael and M. J. Donahue, Physica B **233**, 272 (1997).
- [11] M. J. Donahue, D. G. Porter, R. D. McMichael, and J. Eicke, J. Appl. Phys. **87**, 5520 (2000).

FIGURES

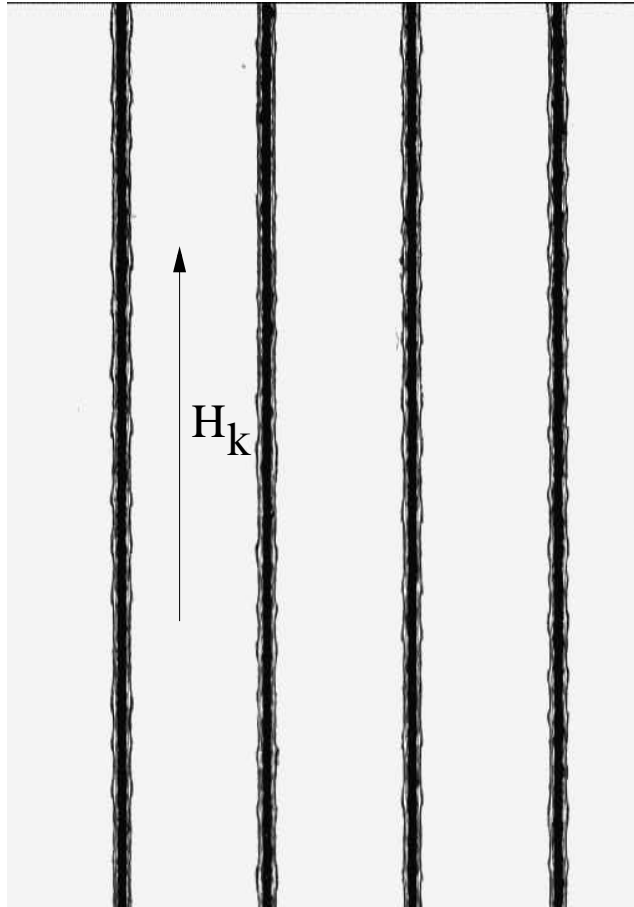


FIG. 1. Micrograph of the patterned layer. Dark zones correspond to ablated regions. Directions of the driving field and the anisotropy axis are indicated.

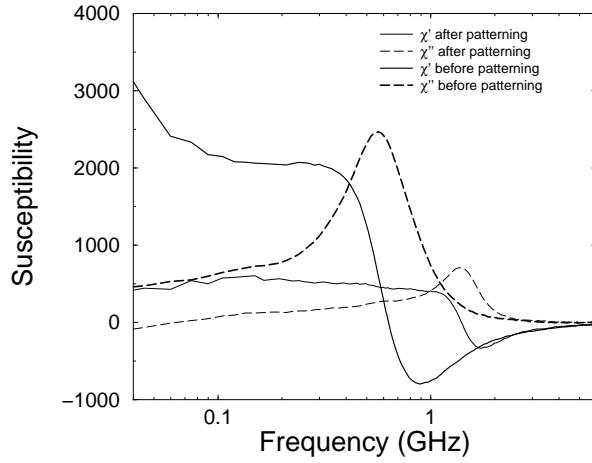


FIG. 2. Susceptibility spectrum before and after patterning, real part ( $\chi'$ ) and imaginary part ( $\chi''$ ). The patterned sample has permalloy stripes  $75 \mu\text{m}$  across separated by  $10 \mu\text{m}$  wide non-magnetic stripes.

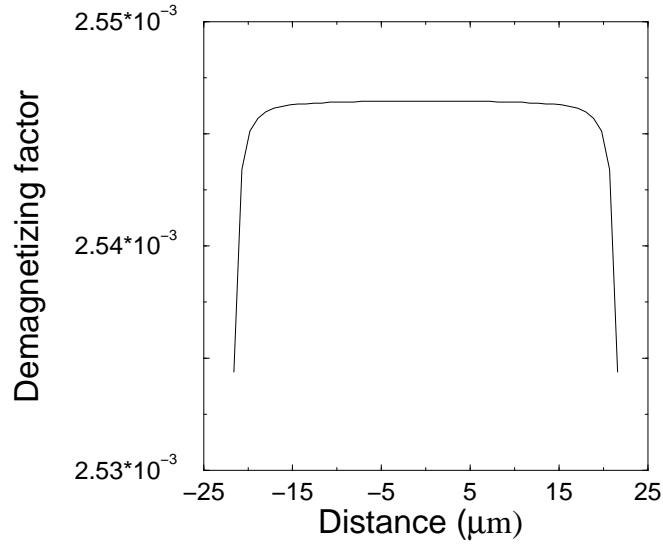


FIG. 3. Demagnetizing factor  $N_y$  for a  $50 \mu\text{m}$  wide stripe, evaluated across the width, along the center line  $x=z=0$ . The origin of the coordinates is taken in the center of the stripe

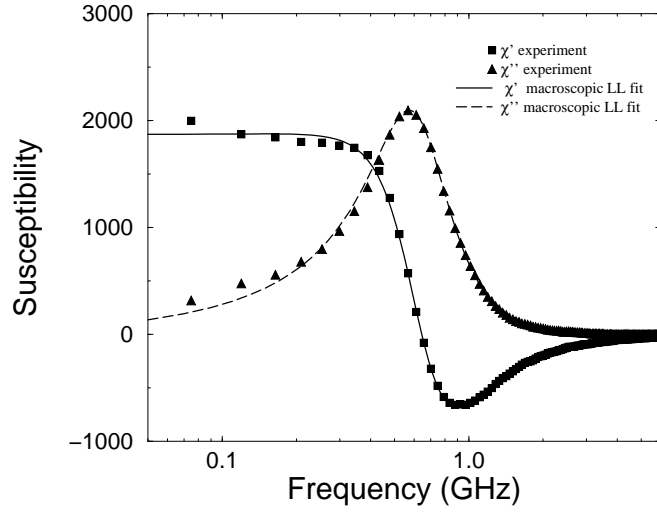


FIG. 4. Fit of experimental susceptibility spectrum by the macroscopic LL model for permalloy. The values of  $H_k$  and  $M_S$  are determined by static measurements ( $H_k = 412 \text{ A} \cdot \text{m}^{-1}$ ,  $M_S = 712000 \text{ A} \cdot \text{m}^{-1}$ ). The value of the damping parameter  $\alpha$  is taken as a free parameter ( $\alpha = 0.021$ ).

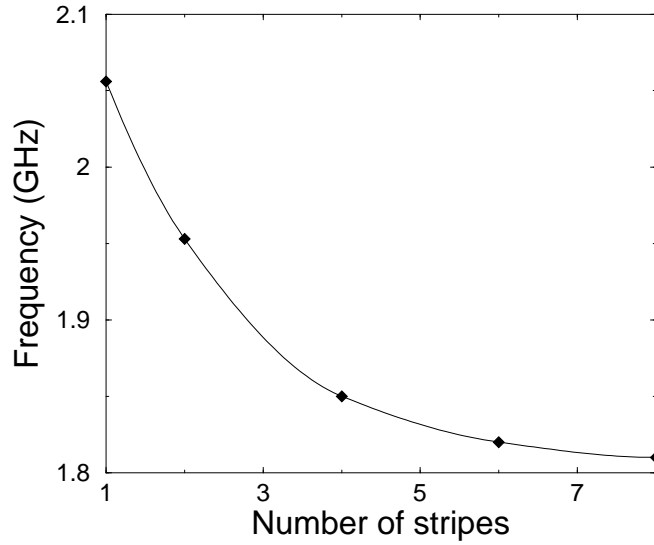


FIG. 5. Calculated resonance frequency as a function of the number of stripes.

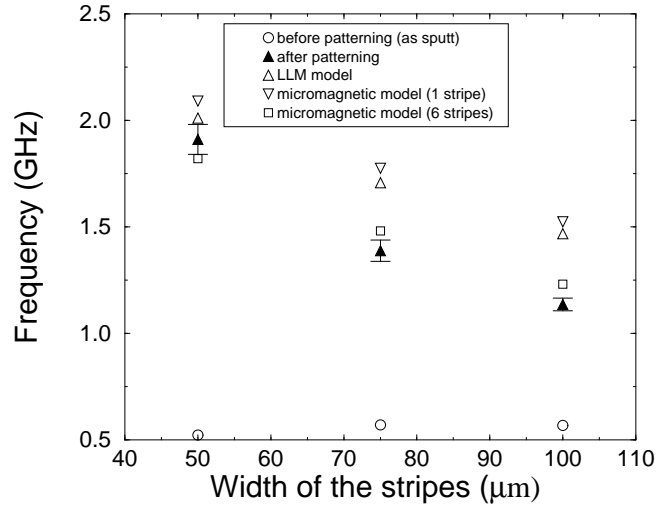


FIG. 6. Evaluation of the gyromagnetic resonance frequency with width of the stripes: experiment, macroscopic LL model and micromagnetic computations.

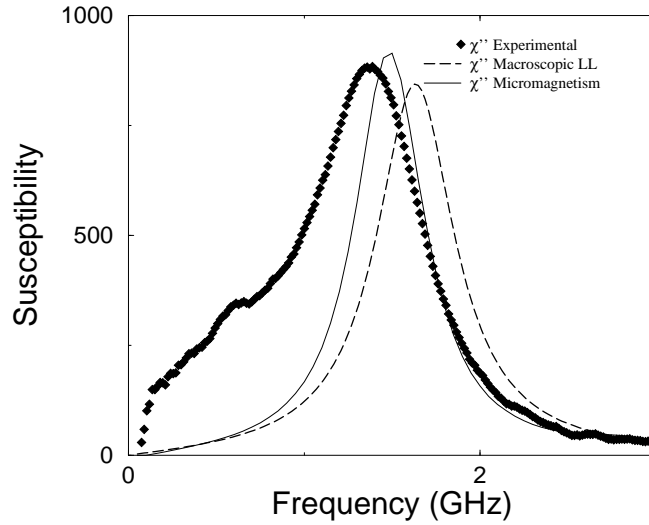


FIG. 7. Imaginary part of the susceptibility spectrum, for experiment, macroscopic LL model and micromagnetic computations.